Inverse beta decay and coherent elastic neutrino nucleus scattering – a comparison

Maitland Bowen[1, 2, *] and Patrick Huber[1, †]

[1] *Center for Neutrino Physics, Virginia Tech, Blacksburg, VA 24061*
[2] *University of Michigan, Ann Arbor, MI, 48109*

(Dated: July 26, 2019)

Many neutrino experiments involving low-energy neutrinos rely on inverse beta decay (IBD), including those studying neutrino oscillations at nuclear reactors, and for applications in reactor monitoring and the detection of neutrinos emitted from spent nuclear fuel. IBD reactions can occur only for electron antineutrinos with energy above a threshold of 1.806 MeV. Below this threshold, the signature of neutrinos is accessible via coherent elastic neutrino-nucleus scattering (CEνNS), a threshold-less reaction. CEνNS was observed for the first time in 2017 at 6.7σ confidence level after forty years of experimentation, albeit with neutrinos of about 10 times larger energy than those from reactors. Here we assume also that neutrinos from reactors and other MeV-sources eventually will be detected using CEνNS. In this paper, we use neutrino fluxes measured from reactors and their cross sections to compute the energy spectra of ^{235}U, ^{238}U, ^{239}Pu, and ^{241}Pu, and determine and compare neutrino detection event counts using either IBD or CEνNS. This characterization will inform future detector choices and is directly applicable to various neutrino sources, including reactor neutrinos, spent fuel neutrinos, and geoneutrinos. The result is potentially useful in monitoring spent nuclear fuel and reactors, in support of nuclear nonproliferation safeguards objectives.

I. INTRODUCTION

Neutrinos were discovered by Cowan and Reines in 1956 [1]. Characterized by their very small probability of interaction with other matter, their detection therefore requires large target masses. Their observation provides insight not only into neutrino properties and particle physics, but into the source of the neutrinos. These sources include supernovae [2], solar neutrinos [3], atmospheric neutrinos [4], cosmic rays [5], and geoneutrinos [6], as well as artificial sources including particle accelerators [7] and nuclear reactors [8].

Inverse beta decay (IBD) is an important process commonly used to study lower-energy neutrinos of less than 60 MeV [9] and is used in most reactor experiments. IBD describes an electron antineutrino scattering off a proton and producing a neutron and positron

$$\bar{\nu}_e + p \to n + e^+ \,. \tag{1}$$

Neutrinos can be detected by IBD only above the threshold energy dictated by the masses of the positron, neutron, and proton. In the laboratory frame, the proton is at rest, and the threshold as expressed in Ref. [9] is

$$E_\nu^{thr} = \frac{(M_N + m_{e^+})^2 - M_p^2}{2M_p} = 1.806 \text{ MeV} \,. \tag{2}$$

Coherent elastic neutrino-nucleus scattering (CEνNS) was postulated soon after neutrino-quark coupling through neutral Z bosons, an implication of the discovery of the weak neutral current. CEνNS occurs between an antineutrino of any flavor and a target nucleus [10]

$$\bar{\nu} + X \to \bar{\nu} + X \,.$$

CEνNS is such a promising detection method for low-energy neutrinos due to its cross section's N^2 dependence, where N is the number of nucleons in the target mass. By one estimate, the CEνNS cross section is approximately three orders of magnitude larger than that of IBD [11], making it the largest of all low-energy neutrino interactions. Despite its high cross section, CEνNS evaded detection for decades because of the difficulty in detecting very low nuclear recoil energies. In 2017, the COHERENT collaboration used a 14.6kg CsI[Na] scintillator to observe CEνNS for the first time from the Spallation Neutron Source at Oak Ridge National Laboratory [12]. COHERENT is currently in the process of deploying four detector subsystems to continue to test the N^2 dependence of the cross section [13].

* mebowen@umich.edu
† pahuber@vt.edu

Applications of IBD and CEνNS

Nuclear nonproliferation safeguards

Physicists in the Soviet Union in 1978 first proposed the use of neutrinos for remote monitoring of nuclear reactors [14]. The typical mixture of isotopes undergoing fission in any reactor is comprised of ^{235}U, ^{238}U, ^{239}Pu, and ^{241}Pu. Both plutonium isotopes are produced by neutron capture on the uranium isotopes. More plutonium is produced the longer and the higher the power at which the reactor runs. Each of these isotopes also has well-defined and unique neutrino emissions, both in the energy spectra and the number of neutrinos emitted. As shown in Fig. 1, the spectrum of weapons-usable ^{239}Pu has the lowest mean energy of the four isotopes within the reactor. The number of neutrinos emitted for each isotope is also shown in Tab. I. By observing the number of neutrinos emitted by reactors and the spectra of those neutrinos, the composition of the reactor fuel and the power level of the reactor can be determined. As a result, one can deduce whether the reactor could potentially be producing weapons-grade material, even without access to records of the reactor history [15]. Analyses with individual reactors have demonstrated that this method of safeguards would have quickly provided information as to the plutonium production in the Democratic People's Republic of Korea during the North Korean nuclear crisis of 1994, given the limited access inspectors were given to the reactor [8]. Studies have also applied this method to IR-40, the Iranian heavy water reactor at Arak, and demonstrated that a neutrino detector can meet or exceed the verification goals set by the International Atomic Energy Agency (IAEA) [16].

Spent nuclear fuel

The rise of nuclear power over the last seven decades has created significant quantities of nuclear waste. With this comes the responsibility of proper management of the highly radioactive spent fuel. Neutrino monitoring via IBD can be used for verification of the contents of dry storage casks above ground; remote monitoring of long-term underground repositories; detecting leaks in storage tanks; and remote sensing of radioactive spills [17].

Geoneutrinos

The Kamioka liquid scintillator antineutrino detector (KamLAND) obtained the first measurements of neutrinos produced within the Earth. The majority of geoneutrinos are electron antineutrinos originating from ^{40}K, ^{232}Th, and ^{238}U. Only the ^{232}Th and ^{238}U decay chains produce neutrinos above the IBD detection threshold. The detection of neutrinos from ^{40}K decay could be possible with CEνNS detectors and would be of great interest to geophysicists, with potential applications to geomagnetism [6].

Neutrino properties

Theoretical and experimental projects have resulted in interest in CEνNS from a variety of fields, compiled by Akimov *et. al.* [12]. CEνNS background from solar and atmospheric neutrinos is an irreducible background in the search for weakly interacting massive particles (WIMPs) as dark matter. Astrophysicists expect that CEνNS dominates neutrino transport during stellar collapse and in neutron stars. CEνNS is an excellent tool in searches for sterile neutrinos, a neutrino magnetic moment, and interactions via new particles beyond the standard model. It also may allow for improved constraints on the weak nuclear charge value and probes of nuclear structure.

II. METHODS

IBD event counts and spectra

To compute the neutrino counts and energy spectra from IBD, we use the cross section calculated in Ref. [9] and the antineutrino fluxes for ^{235}U, ^{238}U, ^{239}Pu, and ^{241}Pu calculated in Ref. [18]. The total cross section at zeroth order can be expressed as

$$\sigma = \frac{2\pi}{m_e^5 f^R \tau_n} E_e p_e \tag{3}$$

where τ_n is the measured neutron lifetime and f^R=1.7152 is the phase space factor [9]. The cross section for IBD is on the order of $10^{-42}\,\text{cm}^2$.

We compute the neutrino yield for each isotope through numerical integration

$$y_I^{IBD} = \int_{0.125\ \text{MeV}}^{8\ \text{MeV}} \sigma_{IBD}(E_\nu) f_I(E_\nu)\, dE_\nu\,. \tag{4}$$

Here, $\sigma_{IBD}(E_\nu)$ represents the IBD cross sections and $f_I(E_\nu)$ represents the neutrino fluxes. We impose a linear interpolation throughout the cross section and flux values and choose to integrate over 0.25 MeV-wide energy bins. We repeat this calculation for each of ^{235}U, ^{238}U, ^{239}Pu, and ^{241}Pu. We then impose a normalization factor

$$N_I = t\frac{P}{E_I} M N_A \frac{2}{14}\frac{1}{4\pi L^2} \tag{5}$$

where t is time, P is reactor power, E_I is the energy per fission, M is the mass of the detector target, and L is the distance from the reactor core. For our calculations, we chose to demonstrate a 1 GW_{th} reactor with a 1 kg CH_2 detector 10 m away from the reactor core for one year. CH_2 is an ideal target, as hydrocarbons have a high number of protons with which neutrinos interact [15]. We also assume the energy per fission to be E_I=200 MeV. Then the number of neutrinos detected is simply $n_I^{IBD} = N_I y_I^{IBD}$. The results are shown in Tab. I.

To compute the neutrino spectra, we return to our numerical integration routine. The value of the integral constrained within each energy bin produces the spectra for each isotope within the reactor. As shown in Fig. 1, peaks for thermal neutron fission in ^{235}U, ^{239}Pu, and ^{241}Pu occur around 3.5 MeV, while the peak for fast neutron fission in ^{238}U occurs around 4 MeV.

CEνNS event counts

The observation of CEνNS opens up a new realm of possibility for neutrino detection, including for reactor neutrinos. While the cross section for IBD interactions can be quite simply expressed as a function of neutrino energy, the CEνNS scattering cross section is differential [11]

$$\frac{d\sigma}{dT}(E_\nu) = \frac{G_F^2}{4\pi} N^2 M_N \left(1 - \frac{M_N T}{2E_\nu^2}\right) \tag{6}$$

where M_N is the atomic weight and N is the number of neutrons in the target nuclei. Similarly to the IBD process, we compute the following integral using the neutrino fluxes

$$\int\int_{T_{min}}^{T_{max}} f_I(E_\nu)\frac{d\sigma}{dT}(E\nu)\, dT\, dE_\nu\,. \tag{7}$$

Here T_{max} and T_{min} are the maximum and minimum nuclear recoil energies, respectively. We calculate event counts with various values for T_{min}. T_{max} is a function of energy [11]

$$T_{max} = \frac{E_\nu}{1 + \frac{M_N}{2E_\nu}}\,. \tag{8}$$

The definite integral is easily solved analytically, and we again use a numerical integration routine over the neutrino energy, again choosing a bin size of 0.25 MeV. We also must ensure that when values of T_{max} at low energies fall below the threshold energy T_{min}, the value of the integral at that point is zero. We then normalize our values again, though we now modify each normalization value for the atomic weight of each potential target nuclei. We repeat this for different threshold energies T_{min} and for each of the potential target isotopes in the detector. The resulting neutrino counts are shown in Tab. II.

III. RESULTS

As seen in Tab. I, the number of neutrinos produced by and detected from each isotope in a reactor differs significantly. At approximately 3000 events with our given parameters, ^{239}Pu produces the fewest neutrinos, at only about two-thirds the rate of ^{238}U. ^{239}Pu also has the lowest mean energy; ^{238}U has the highest mean energy, which

Isotope	^{239}Pu	^{241}Pu	^{235}U	^{238}U
Events	3000	4160	4360	6580

TABLE I. IBD event number per kg of CH_2 per year at a 1 GW_{th} reactor and at a distance of 10 m.

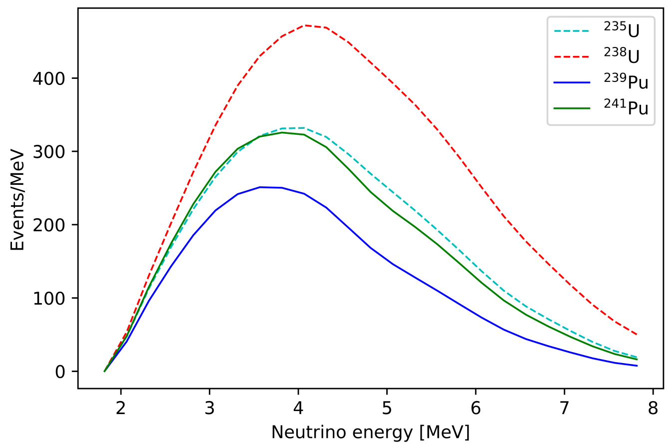

FIG. 1. Energy spectra for uranium-235, uranium-238, plutonium-239, and plutonium-241.

also peaks at a higher energy value than the other three isotopes, as shown in Fig. 1. With observations of both the event number and the spectra of the neutrinos emitted from a nuclear reactor, one can deduce both the composition of the mixture within the reactor and the power level of the reactor itself. This can allow for detection of potentially weapons-grade plutonium-239, and therefore can serve as an important safeguard against nuclear nonproliferation.

Table II shows the neutrino event number above a given nuclear recoil energy threshold for various isotopes that could serve as target masses in detectors for CEνNS.

Threshold [eV]	Isotope ^{4}He	^{12}C	^{20}Ne	^{28}Si	^{40}Ar	^{74}Ge	^{127}I	^{132}Xe	^{133}Cs
0	4360*	13100	21800	30500	52800	104000	188000	201000	200000
10	4320*	12800	20900	28900	48900	91000	152000	161000	160000
100	4030*	10700	15900	20200	30400	42200	47200	48400	47600
1 000	2510*	3480*	3030*	2330*	1710*	294*	0.719*	0.185*	0.123*
10 000	141*	0.239*	0.00*	0.00*	0.00*	0.00*	0.00*	0.00*	0.00*

TABLE II. CEνNS event number per kg per year for Uranium-235 at a 1 GW_{th} reactor and at a distance of 10 m as a function of isotope and recoil energy threshold. The corresponding event number for IBD in 1 kg of CH_2 is 4360, as shown in Tab. I. Event numbers lower than this are marked with an asterisk.

Almost every potential target isotope we considered will detect fewer neutrinos than a currently operating IBD detector if the CEνNS detector is unable to observe recoil energies below the order of 1 keV.

Table III shows the recoil energies at which a CEνNS detector with the given isotope as a target will detect the same number of neutrinos as IBD. This is again using the parameters outlined previously with respect to reactor power, observation time, distance, and target mass for ^{235}U. For example, germanium-74, a common target material in neutrino detectors, will detect fewer neutrinos than a currently operating IBD detector if the CEνNS detector is unable to observe recoil energies below the required 491 eV. Table III also demonstrates the linearity of the threshold energy versus the mass number of the target.

Isotope	^{4}He	^{12}C	^{20}Ne	^{28}Si	^{40}Ar	^{74}Ge	^{127}I	^{132}Xe	^{133}Cs
Threshold [eV]	0	790	770	702	672	491	353	347	343

TABLE III. The recoil energy threshold at which IBD and the CEνNS detector parameters described in Tab. II result in the same neutrino event number

The same challenge that allowed CEνNS to evade detection for forty years dictates the efficacy of its use in experimental neutrino physics. The potential for drastically increased neutrino counts using CEνNS is a very real one, but only when our detector technology catches up to theory. Great advances have been made to detect the very small recoil energies of CEνNS, and with continued advancement, CEνNS will offer improved opportunities for new understandings of neutrino physics.

ACKNOWLEDGEMENTS

The work of MB was supported by the National Science Foundation REU grant number 1757087. The work of PH was supported by the US Department of Energy Office of Science under award number DE-SC00018327.

---

[1] C. L. Cowan, F. Reines, F. B. Harrison, H. W. Kruse, and A. D. McGuire, "Detection of the free neutrino: a confirmation," Science **124**, 103–104 (1956), http://science.sciencemag.org/content/124/3212/103.full.pdf.

[2] K. Hirata, T. Kajita, M. Koshiba, M. Nakahata, Y. Oyama, N. Sato, A. Suzuki, M. Takita, Y. Totsuka, T. Kifune, T. Suda, K. Takahashi, T. Tanimori, K. Miyano, M. Yamada, E. W. Beier, L. R. Feldscher, S. B. Kim, A. K. Mann, F. M. Newcomer, R. Van, W. Zhang, and B. G. Cortez, "Observation of a neutrino burst from the supernova sn1987a," Phys. Rev. Lett. **58**, 1490–1493 (1987).

[3] Alain Bellerive, "Review of solar neutrino experiments," *Proceedings, 21st International Symposium on Lepton and Photon Interactions at High Energies (LP 03): Batavia, ILL, August 11-16, 2003*, Int. J. Mod. Phys. **A19**, 1167–1179 (2004), arXiv:hep-ex/0312045 [hep-ex].

[4] Fukuda Y. *et al.* (Super-Kamiokande Collaboration), "Evidence for oscillation of atmospheric neutrinos," Phys. Rev. Lett. **81** (1998), 10.1103/PhysRevLett.81.1562.

[5] Francis Halzen and John Learned, "High energy neutrino detection in deep polar ice," in *Proceedings of the 5th International Symposium on Very High Energy Cosmic Ray Interactions, Lodz, Poland*, MAD/PH/428, UH-511-659-88 (University of Wisconsin, Madison, 1988).

[6] T. Araki *et al.*, "Experimental investigation of geologically produced antineutrinos with KamLAND," Nature **436**, 499–503 (2005).

[7] Ubaldo Dore, Pier Loverre, and Lucio Ludovici, "History of accelerator neutrino beams," (2018), arXiv:1805.01373 [physics.acc-ph].

[8] Eric Christensen, Patrick Huber, and Patrick Jaffke, "Antineutrino reactor safeguards - a case study," Science and Global Security **23**, 20–47 (2015), arXiv:1312.1959 [physics.ins-det].

[9] P. Vogel and John F. Beacom, "Angular distribution of neutron inverse beta decay, anti-neutrino(e) + p —¿ e+ + n," Phys. Rev. **D60**, 053003 (1999), arXiv:hep-ph/9903554 [hep-ph].

[10] Daniel Z. Freedman, "Coherent Neutrino Nucleus Scattering as a Probe of the Weak Neutral Current," Phys. Rev. **D9**, 1389–1392 (1974).

[11] Bernadette K. Cogswell and Patrick Huber, "Detection of breeding blankets using antineutrinos," Science & Global Security **24**, 114–130 (2016), https://doi.org/10.1080/08929882.2016.1184531.

[12] D. Akimov *et al.* (COHERENT), "Observation of Coherent Elastic Neutrino-Nucleus Scattering," Science **357**, 1123–1126 (2017), arXiv:1708.01294 [nucl-ex].

[13] D. Akimov *et al.* (COHERENT), "COHERENT 2018 at the Spallation Neutron Source," (2018), arXiv:1803.09183 [physics.ins-det].

[14] A. A. Borovoi and L. A. Mikaelyan, "Possibilities of the practical use of neutrinos," Soviet Atomic Energy **44**, 589 (1978).

[15] Rachel Carr *et al.*, "Neutrino-based tools for nuclear verification and diplomacy in North Korea," (2018), arXiv:1811.04737 [physics.soc-ph].

[16] Eric Christensen, Patrick Huber, Patrick Jaffke, and Thomas E. Shea, "Antineutrino Monitoring for Heavy Water Reactors," Phys. Rev. Lett. **113**, 042503 (2014), arXiv:1403.7065 [physics.ins-det].

[17] Vedran Brdar, Patrick Huber, and Joachim Kopp, "Antineutrino monitoring of spent nuclear fuel," Phys. Rev. Applied **8**, 054050 (2017), [Phys. Rev. Applied.8,054050(2017)], arXiv:1606.06309 [hep-ph].

[18] Patrick Huber, "On the determination of anti-neutrino spectra from nuclear reactors," Phys.Rev. **C84**, 024617 (2011), arXiv:1106.0687 [hep-ph].